ChemComm

COMMUNICATION

View Article Online
View Journal | View Issue

Cite this: *Chem. Commun.*, 2016, 52, 4301

Received 29th November 2015,
Accepted 23rd February 2016

DOI: 10.1039/c5cc09859a

www.rsc.org/chemcomm

A novel dimethylformamide (DMF) free bar-cast method to deposit organolead perovskite thin films with improved stability†

Eurig W. Jones,[a] Peter J. Holliman,*[a] Arthur Connell,[a] Matthew L. Davies,[b] Jennifer Baker,[b] Robert J. Hobbs,[a] Sanjay Ghosh,[a] Leo Furnell,[a] Rosie Anthony[a] and Cameron Pleydell-Pearce[b]

We report a solvent-free approach to synthesizing organolead perovskites by using solid state reactions to coat perovskite crystals onto Al_2O_3 or TiO_2 nanoparticles followed by addition of terpineol affording perovskite inks. We have bar cast these inks to produce photoactive perovskite thin films which are significantly more stable to humidity than solution-processed films. This new method also avoids the use of toxic DMF solvent.

Since the initial reports of organolead halide perovskite solar cells,[1,2] device efficiencies have risen rapidly towards 20%.[3] It has also been demonstrated that such perovskites work efficiently in a variety of PV device architectures[4] including planar TiO_2 charge collection layers[5] and mesoporous TiO_2 as well as in batteries[6a] and sensors.[6b] Electrically-insulating Al_2O_3 scaffolds[1] and even hole transporter-free perovskite devices[7] have been reported, demonstrating that the perovskite absorber layer can efficiently sustain charge transport. This is important because key limiting factors for perovskite solar cells are the surface coverage and crystallisation steps which occur at the perovskite–metal oxide interface during device manufacture. As a result, perovskite device manufacturing is the subject of much interest. A current limitation for one-step, solution processed perovskites is infiltration into the mesoporous scaffold, which can be improved by sequential deposition,[8] affording superior coverage and avoiding the need for a perovskite capping layer. However, concerns remain over the solvents used for solution processed perovskites[9] and the stability of the resulting materials to temperature and/or moisture.[10,11] As such, recent reports suggest optimum fabrication conditions such as %RH $< 1\%$[10] which complicates scale up.

To date, the choice of perovskite processing solvent has been limited to dimethylformamide (DMF),[1] dimethylsulfoxide (DMSO)[12] or γ-butyrolactone (GBL)[2] given the need to dissolve the PbX_2 precursor (X = Cl, Br, I). By comparison, methyl ammonium halides are readily soluble in most solvents including water. In this paper, we report that a 1 : 1 ratio of PbX_2 and CH_3NH_3X react readily together with quantitative yield in solvent-free, solid state reactions by grinding/milling (ESI,† Fig. S1). We have also studied the addition of metal oxide nanoparticles (Al_2O_3 or TiO_2) as common scaffold materials for perovskite solar cells during or after the solid state perovskite reaction. After perovskite has formed on the metal oxide surface, to produce a printable ink, we have ground the particles in terpineol as a suspending media rather than a solvent. Perovskite crystals have previously been suspended in DMF[12] but here terpineol has been chosen because it has low toxicity and is widely used in printing media. It also possesses a high boiling point (219 °C), which is similar to DMSO (189 °C) which has been reported to stabilise solvent–PbI_2 complexes and inhibit PbI_2 crystallization.[13] This also avoids the DMF volatilisation (b.p. 153 °C) during spin coating, which increases perovskite crystal dislocations. Higher boiling solvents also encourage slower perovskite crystal growth during annealing. The resultant inks can then be doctor bladed or bar cast. We have studied the influence of metal oxide loading and found that, for Al_2O_3, a loading of $>10\%$ Al_2O_3 is required to cast a uniform layer, presumably because Al_2O_3 acts as a plasticizer. This is more than the 5% Al_2O_3 reported by Carnie *et al.*[14] for their DMF/perovskite/Al_2O_3 nanoparticle precursor in their spin coating based study. The difference is that the perovskite particles are pre-formed on the Al_2O_3 particle surfaces in our inks and no DMF is present unlike previous reports of bar-cast perovskites.[15] Visual inspection also suggests that the resulting colloidal inks are stable for >3 months. An additional advantage of developing inks for meso-scopic perovskite solar cells using a passive Al_2O_3 scaffold is their low-temperature processability. Thus, our inks can be deposited under ambient conditions and heated at 110 °C because high temperature processing is not required to ensure inter-particle "necking" to carry electrical charge as is the case for TiO_2 photo-electrodes.[16] This is in line with previous reports for Al_2O_3 where heat processing is shown

[a] School of Chemistry, Bangor University, Bangor, Gwynedd LL57 2UW, UK
[b] SPECIFIC, Swansea University, Swansea, SA1 8EN, UK.
E-mail: p.j.holliman@bangor.ac.uk

† Electronic supplementary information (ESI) available. See DOI: 10.1039/c5cc09859a

to be complete at 150 °C[17] and 110 °C.[14] The perovskite ink formation is described in eqn (1) and (2).

$$[PbX_2 + Al_2O_3] + CH_3NH_3X \rightarrow [CH_3NH_3PbX_3 : Al_2O_3] \quad (1)$$

$$[CH_3NH_3PbX_3 : Al_2O_3] + \text{terpineol} \rightarrow \text{Perovskite ink} \quad (2)$$

For film deposition, a compact 80 nm TiO_2 layer (Solaronix BL) was spin coated (3500 rpm, 60 s) onto TEC15 glass (15 Ω sq^{-1}, NSG) and heated (550 °C for 1 h). Perovskite inks were deposited onto these substrates either by spin coating, doctor blading or bar casting to produce films ranging from 400 nm to *ca.* 10 μm in thickness. In addition, to drastically increasing the atom efficiency of the perovskite manufacturing process, the stoichiometric nature of these solid state reactions is key to improving the compositional control over the materials produced. Thus, in Snaith *et al.* original report of perovskite devices,[1] a 3 : 1 ratio of $CH_3NH_3I : PbCl_2$ was used along with spin coating to control layer thickness. However, the I : Cl ratio of the resultant $CH_3NH_3PbI_2Cl$ was reported as 2 : 1. Effectively, this means that an excess of CH_3NH_3I is required to convert all the $PbCl_2$ into perovskite. Whilst CH_3NH_3X waste is less of an issue at the laboratory scale, it is not viable for a scaled process because it multiplies raw material costs and environmental impact which has been reported to be greater for CH_3NH_3I than for PbX_2.[18] By comparison, in the solid state reactions, CH_3NH_3X and PbX_2 can be reacted together in the desired ratio and this ratio is carried through into the resulting perovskite material. A further advantage of solid state reactions is much greater control of trace components (*e.g.* Cl^-) which is known to be key to device performance.[19]

To prepare organolead perovskites on Al_2O_3, PbX_2 (X = Cl, Br, I) and Al_2O_3 nanoparticles (mean size 13 nm) are ground together until there is no further colour change. After adding the desired CH_3NH_3X to this the mixture is ground together again. Conversion to a perovskite phase varies depending on the halides used. For $CH_3NH_3PbI_{3-x}Cl_x$, an intermediate non-perovskite yellow phase is obtained (Fig. 1b) which only turns black and converts to perovskite after heating at 120 °C for 50 min (*i.e.* standard solution processing conditions). A similar intermediate perovskite complex, has been previously reported by Wu *et al.*[13] By comparison, the $CH_3NH_3PbI_3$ ink turns black purely by mechanical mixing and before heating at 120 °C (Fig. 1a). We have defined the pre-heated tri-iodide as ''semi-perovskite'' ink as the XRD data confirm significant amounts of unconverted PbI_2 are still present, which then decrease after heating. Finally, $CH_3NH_3PbBr_3$ turns orange on grinding which fully converts and increases in crystallinity on heating (ESI,† Fig. S3). Upon the addition of terpineol, each reaction continues to completion and we believe the terpineol assists in a wet grinding process whereby the size of the PbX_2 and CH_3NH_3X crystals are further reduced and these particles are more intimately mixed enabling intercalation of CH_3NH_3X into the lead halide lattice to form crystalline perovskite.

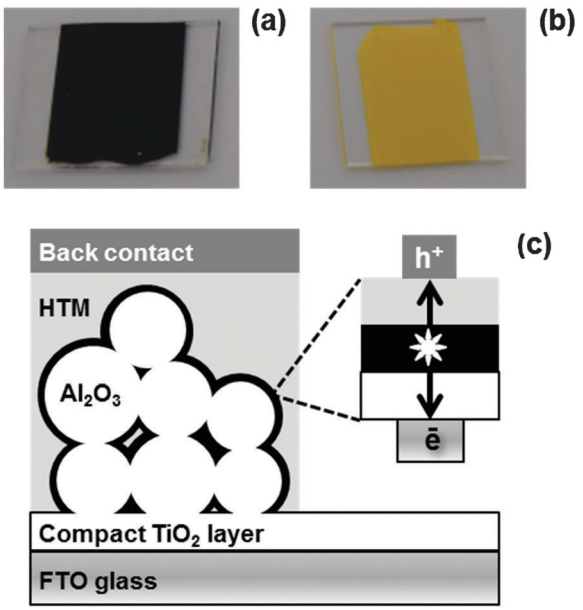

Fig. 1 (a) Semi-perovskite, (b) perovskite intermediate and (c) schematic of perovskite device architecture.

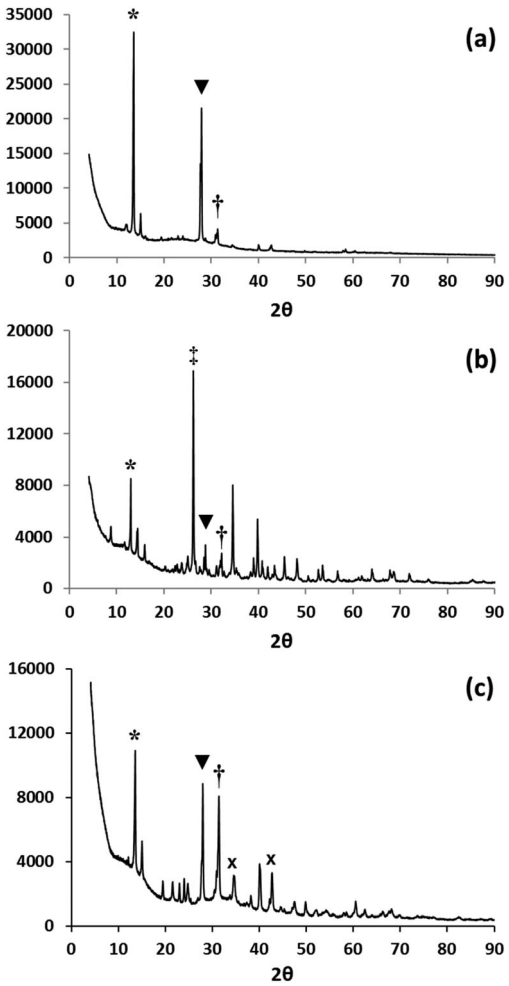

Fig. 2 XRD data of $CH_3NH_3PbI_3$ films manufactured by (a) solution processing, (b) solid state reaction using TiO_2 and (c) deposited on glass from a perovskite ink. * (110), (220), † (310) of perovskite phase, × (Al_2O_3), ‡ (101) TiO_2 diffraction lines.

X-Ray powder diffraction data show that the solid state reaction between CH_3NH_3I and PbI_2 produces predominantly the $CH_3NH_3PbI_3$ phase with only low intensity peaks observed for PbI_2 (Fig. 2b). Unconverted PbI_2 has been reported previously in the two-step solution processing method, even when the substrate is heated to 60 °C, to constrain lateral crystal growth.[20] The PbI_2 peaks observed in our work (ground samples) more closely resemble data observed for samples deposited on optimally pre-heated (50 °C) substrates, which is typically done to assist small particle formation and improve coverage.[13] After grinding in terpineol (Fig. 2c), the (110) peak for the perovskite phase increases in relative intensity, confirming that the solid state reaction continues on further grinding in the solvent. Data from line broadening suggest that the average crystal/domain size is *ca.* 100 nm which is similar to that typically observed purely for one-step solution processing methods rather than the larger 500 nm particle sizes observed using the two-step method.[17] In addition for both ground samples, there is less evidence of preferred orientation (Fig. 2b and c) compared to solution deposited material (Fig. 2a). This is to be expected as the solution deposited samples nucleate and grow directly onto a flat substrate which is heated from below making perpendicular crystal growth much more likely. By comparison, the ground samples nucleate and crystallise onto randomly oriented metal oxide particles so the orientation of their crystal growth will also be randomised.

Photoluminescence (PL) of perovskite films is strongly linked to device efficiency[21] and so PL microscopy and *in situ* spectroscopy of perovskite:metal oxide films was carried out to evaluate surface coverage and electron shuttling. The data show that films of doctor bladed $CH_3NH_3PbI_{3-x}Cl_x$, bar cast $CH_3NH_3PbI_{3-x}Cl_x$ and $CH_3NH_3PbBr_3$ are all emissive, which suggests they should all be photo-active in PV devices (Fig. 3a–c). As expected, the thicker 7 μm doctor bladed $CH_3NH_3PbI_{3-x}Cl_x$ film (Fig. 3a and f) shows PL intensity which is much greater than that of the equivalent 400 nm bar cast film (Fig. 3b and f). Interestingly, the intensity of the doctor bladed film is comparable to the solution processed image (Fig. 3e and f). In terms of coverage, two issues need consideration. Firstly, there is the coverage of the mesoporous Al_2O_3 film on the substrate and secondly there is the coverage of the perovskite layer on the Al_2O_3 surface. For the doctor bladed film, the perovskite coverage on the Al_2O_3 surface appears to be consistent whilst the mesoporous Al_2O_3 film is much less even. However, there do not appear to be any pin holes in this film which would cause short circuiting in PV devices made from this material. By comparison, the coverage of the perovskite on the Al_2O_3 surface in the bar coated film appears less complete although the mesoporous Al_2O_3 film itself still appears to be complete. For the analogous bar coated $CH_3NH_3PbBr_3$ sample, greater PL intensity is observed than for the $CH_3NH_3PbI_{3-x}Cl_x$ sample although at λ ca. 540 nm reflecting the larger band gap for the tribromide perovskite. Here, the perovskite coverage on Al_2O_3 seems fairly complete although some areas seem brighter than others suggesting variable particle sizes of perovskite crystals have been deposited (Fig. 3c). To further study scaffold coverage, a TiO_2-based $CH_3NH_3PbI_3$ paste was bar coated onto a glass substrate. The maximum PL

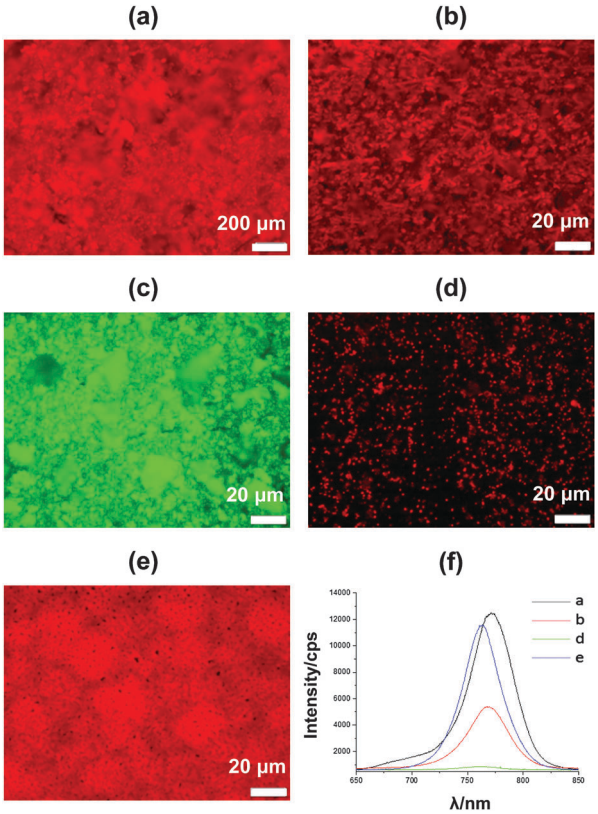

Fig. 3 Photoluminescence images of films of (a) 7 μm, 2-step, doctor bladed $CH_3NH_3PbI_{3-x}Cl_x$, (b) 4 μm wet thickness, bar cast sequential $CH_3NH_3PbI_{3-x}Cl_x$, (c) 4 μm wet thickness, bar cast $CH_3NH_3PbBr_3$, (d) 4 μm wet thickness, bar cast, one step TiO_2–$CH_3NH_3PbI_3$, (e) spun coated solution processed $CH_3NH_3PbI_{3-x}Cl_x$ and (f) intensity *vs.* λ for selected PL image.

intensity for this sample is *ca.* 600 cps compared to *ca.* 12 000 cps for the doctor bladed and *ca.* 6000 cps bar coated $CH_3NH_3PbI_{3-x}Cl_x$ films. Firstly, this suggests that the perovskite films formed can effectively inject into an electrically-conducting scaffold whilst the PL mapping (Fig. 3d) of TiO_2-based perovskite ink shows areas of low PL intensity across the film surface. As the films are not under load, we expect emission to be faster than injection so the low emission for this film may reflect poor coverage or lower stability of the $CH_3NH_3PbI_3$ on TiO_2. By comparison, the more uniform emission across the perovskite: Al_2O_3 films confirms better coverage and perovskite stability and could also suggest lower losses at grain boundaries or crystal interfaces where emission might be quenched. Ultimately, assuming that more emission relates to more potential charge extraction in a PV device under load and given the need for PV devices to possess lifetimes of many years this suggests Al_2O_3 scaffolds should be preferable to TiO_2. Furthermore, perovskites which have been solution processed onto metal oxide scaffolds exhibit slightly blue-shifted emission (760 nm *vs.* 750 nm) as a result of confined growth within mesoporous films.[22,23] Fig. 3f shows that the PL peaks of the ink-based films are similarly blue shifted compared to the solution processed film. This suggests that the perovskite crystals from perovskite inks are similar in size to those grown inside scaffolds, using standard solution processed methods

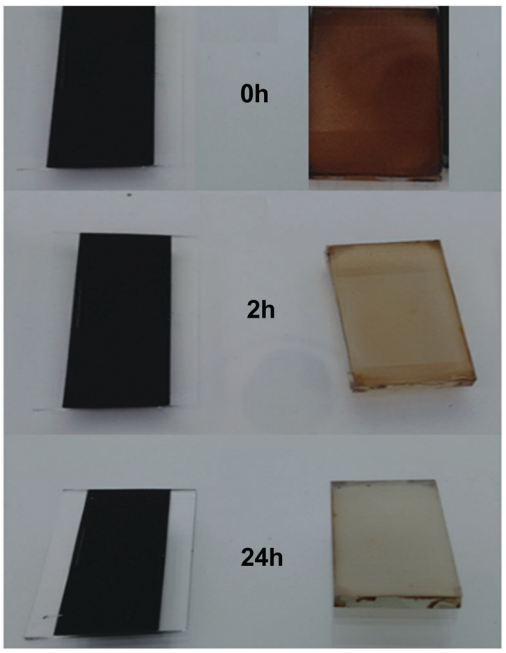

Fig. 4 (left) Bar-cast $CH_3NH_3PbI_3$:Al_2O_3 perovskite ink and (right) spin coated, solution processed $CH_3NH_3PbI_3$ films *vs.* time.

(*i.e.* typically <100 nm). Perovskite film morphology has also been investigated by SEM (ESI,† Fig. S5–S8) which shows the best perovskite coverage for $CH_3NH_3PbBr_3$ ink in line with the higher intensity PL data for this film.

The lifetime of the perovskite films has also been studied (Fig. 4). The data show that Al_2O_3-based films exhibit significantly better resistance to atmospheric exposure (air, humidity, light) than solution processed films. We have observed that the first stage of humidity-driven perovskite degradation involves phase separation into PbX_2 and CH_3NH_3X but that both materials remain on the surface. Hence, in the early stages of degradation, the process can be reversed by heating at 100 °C. However, this reversibility is only possible when the PbX_2 and CH_3NH_3X are proximally located on the surface. As further phase separation occurs with time, this process becomes irreversible by heating. However, it can be reversed by drying, grinding and heating to re-mix the PbX_2 + CH_3NH_3X. Here, we believe that the stabilising influence of the Al_2O_3 is to slow the rate of phase separation and, in doing so, effectively to shift the equilibrium (PbX_2 + CH_3NH_3X ↔ $CH_3NH_3PbX_3$) towards perovskite. Interestingly, Al_2O_3 capping layers on the perovskite absorber layer have also been reported as moisture barriers.[10] TGA data (ESI,† Fig. S11 and S12) suggest that some terpineol may remain after heating but that this reduces with increasing temperature and/or time. If terpineol acts as a solvent of crystallization it should slow H_2O ingress but residual solvent is not expected to limit PV efficiency as it has been reported that small amounts of inert media (*e.g.* PEG[24]) do not limit device performance. However, removing all terpineol does not reduce film lifetime (ESI,† Fig. S12) suggesting surface perovskite:Al_2O_3 interactions may enhance film stability.

In summary, we have demonstrated that photo-active, organo-lead perovskites can be prepared by solid state reactions onto Al_2O_3 scaffolds producing materials with enhanced stability. Whilst this resolves key processing limitations by negating the need for toxic or hygroscopic solvents such as DMF, GBL or DMSO,[9] this approach also makes the synthesis of other (*e.g.* lead-free) organometallic perovskites much simpler as it avoids complex solvent engineering issues[25] or complex solvent–solvent extraction techniques.[26] In addition, using solid state reactions means that all the raw materials end up in the product which makes it easier to add trace components. Also the printing of pre-made perovskite inks is easily scalable whilst solution-based spin coating is not and the vast majority of precursor solutions are spun away making compositional control very difficult.

References

1 M. M. Lee, J. Teuscher, T. Miyasaka, T. N. Murakami and H. J. Snaith, *Science*, 2012, **338**, 643.
2 L. Etgar, P. Gao, Z. Xue, Q. Peng, A. K. Chandriran, B. Liu, M. K. Nazeeruddin and M. Grätzel, *J. Am. Chem. Soc.*, 2012, **134**, 17396.
3 W. S. Yang, J. H. Noh, N. J. Jeon, Y. C. Kim, S. Ryu, J. Seo and S. I. Seok, *Science*, 2015, **348**, 1234.
4 T. Salim, S. Sun, Y. Abe, A. Krishna, A. C. Grimsdale and Y. M. Lam, *J. Mater. Chem. A*, 2015, **3**, 8943.
5 M. Liu, M. B. Johnson and H. J. Snaith, *Nature*, 2013, **501**, 395.
6 (*a*) H.-R. Xia, W.-T. Sun and L.-M. Peng, *Chem. Commun.*, 2015, **51**, 13787; (*b*) C. Muthu, S. R. Nagamma and V. C. Nair, *RSC Adv.*, 2014, **4**, 55908.
7 Y. Jin and G. Chumanov, *ACS Appl. Mater. Interfaces*, 2015, **7**, 12015.
8 N. Yantara, D. Sabba, F. Yanan, J. M. Kadro, T. Moehl, P. P. Boix, S. Mhaisalkar, M. Grätzel and C. Grätzel, *Chem. Commun.*, 2015, **51**, 4603.
9 P. J. Holliman, A. Connell, E. W. Jones, S. Ghosh, L. Furnell and R. J. Hobbs, *Mater. Res. Innovations*, 2016, **19**, 508.
10 J. Burschka, N. Pellet, S. J. Moon, R. Humphry-Baker, P. Gao, M. K. Nazeeruddin and M. Grätzel, *Nature*, 2013, **499**, 316.
11 S. Luo and W. A. Daoud, *J. Mater. Chem. A*, 2015, **3**, 8992.
12 L. C. Schmidt, A. Pertega, S. Gonzalez-Carrero, O. Malinkiewicz, S. Agouram, G. M. Espallargas, H. J. Bolink, R. E. Galian and J. Perez-Prieto, *J. Am. Chem. Soc.*, 2014, **136**, 850.
13 Y. Wu, A. Islam, X. Yang, C. Qin, J. Liu, K. Zhang, W. Peng and L. Han, *Energy Environ. Sci.*, 2014, **7**, 2934.
14 M. J. Carnie, C. Charbonneau, M. L. Davies, J. Troughton, T. M. Watson, K. Wojciechowski, H. Snaith and D. A. Worsley, *Chem. Commun.*, 2013, **49**, 7893.
15 Y. Deng, E. Peng, Y. Shao, Z. Xiao, Q. Dong and J. Huang, *Energy Environ. Sci.*, 2015, **8**, 1544.
16 P. J. Holliman, D. K. Muslem, E. W. Jones, A. Connell, M. L. Davies, C. Charbonneau, M. J. Carnie and D. A. Worsley, *J. Mater. Chem. A*, 2014, **2**(29), 11134.
17 J. M. Ball, M. M. Lee, A. Hey and H. J. Snaith, *Energy Environ. Sci.*, 2013, **6**, 1739.
18 N. Espinosa, L. Serrano-Luján, A. Urbino and F. C. Krebs, *Sol. Energy Mater. Sol. Cells*, 2015, **137**, 303.
19 Q. Chen, H. Zhou, Y. Fang, A. Z. Stieg, T.-B. Song, H.-H. Wang, X. Xu, Y. Liu, S. Lu, J. You, P. Sun, J. McKay, M. S. Goorsky and Y. Yang, *Nat. Commun.*, 2015, **6**, 7269.
20 H.-S. Ko, J.-W. Lee and N.-G. Park, *J. Mater. Chem. A*, 2015, **3**, 8808.
21 F. Deschler, M. Price, S. Pathak, L. E. Klintberg, D.-D. Jarausch, R. Higler, S. Hüttner, T. Leitjens, S. D. Stranks, H. J. Snaith, M. Atatüre, R. T. Phillips and R. H. Friendm, *J. Phys. Chem. Lett.*, 2014, **5**, 1421.
22 M. De Bastiani, V. D'Innocenzo, S. D. Stranks, H. J. Snaith and A. Petrozza, *APL Mater.*, 2014, **2**, 081509.
23 V. D'Innocenzo, G. Grancini, M. J. P. Alcocer, A. R. S. Kandada, S. D. Stranks, M. M. Lee, G. Lanzani, H. J. Snaith and A. Petrozza, *Nat. Commun.*, 2014, **5**, 3586.
24 C.-Y. Chang, C.-Y. Chu, Y.-C. Huang, S.-Y. Chang, C.-A. Chen, C.-Y. Chao and W.-F. Su, *ACS Appl. Mater. Interfaces*, 2015, **7**, 4955.
25 N.-J. Jeon, J.-H. Noh, Y.-C. Kim, W.-S. Yang, S. Ryu and S.-I. Seok, *Nat. Mater.*, 2014, **13**, 897.
26 Y. Zhou, M. Yang, W. Wu, A. L. Vasiliev, K. Zhu and N. P. Padture, *J. Mater. Chem. A*, 2015, **3**, 8179.

